
PERGAMON

Scripta mater. 43 (2000) 935–942

Scripta MATERIALIA

www.elsevier.com/locate/scriptamat

PHASE FIELD MODELING OF SIMULTANEOUS NUCLEATION AND GROWTH BY EXPLICITLY INCORPORATING NUCLEATION EVENTS

J.P. Simmons†, C. Shen* and Y. Wang*
†Air Force Research Laboratory, AFRL/MLLM, Wright-Patterson AFB, OH 45433, USA
*The Ohio State University, 2041 College Road, Columbus, OH 43210, USA

(Received June 22, 1999)
(Accepted in revised form May 10, 2000)

Keywords: Phase transformation; Nucleation; Growth; Ordering; Transport

Introduction

Significant cost savings are realized in alloy processing by using computer models of the processes, reducing the amount of experimental effort necessary. Understanding the mechanisms involved in processing also increases the engineer's level of control over the process. Conventional processing models [1–4] can be used to significantly reduce the costs of process development, but suffer from the limitation of needing large amounts of empirical information for calibration. Physics-based models are expected to have better extrapolative properties and require significantly less information for calibration. One physics-based model that has gained much attention lately is the Phase Field method [5–8], which has been used to simulate microstructural development under site saturation conditions. This work is an attempt to extend the Phase Field method in order to simulate processes involving simultaneous nucleation and growth.

In real processes, isothermal conditions cannot generally be realized because of competing constraints. For example, with parts such as turbine disks, the γ-γ' microstructure must be sufficiently fine after cooling to allow for subsequent heat treatment because resolutionizing will run the risk of causing excessive grain growth. Microstructure formation occurring during cooling usually involves concurrent nucleation and growth because the change in temperature keeps providing additional driving force for nucleation.

The process of concurrent nucleation and growth has been treated theoretically by Langer and Schwartz [9], which calculated the evolution of particle size distributions in near critical fluids, accounting for supersaturation, nucleation of new particles, and capillarity. This treatment was modified by Wendt and Haasen [10], to account for conditions far from a critical point, and later by Kampmann and Wagner, to account for non-linear contributions to capillarity and to eliminate assumptions as to the shape of the particle size distribution [11,12]. A similar approach has been successfully applied to predicting microstructural evolution of Ni-based superalloys by Gabb, *et al*. [13].

The Langer-Schwartz approach gives a particle size distribution as an output, but does not provide additional information such as multipoint correlation functions. Because the Phase Field model simulates whole microstructures, it allows these microstructural statistics to be derived. It has the additional strengths of being able to treat systems with high volume fractions (>50%) and elastic interactions between coherent precipitates and the matrix. In its present form, however, the phase field

PII: S1359-6462(00)00517-0

model handles nucleation only in the site saturation approximation, in which all nuclei form very rapidly, and growth ensues very early on [14].

This work was undertaken in order to adapt the Phase Field model to conditions of concurrent nucleation and growth. This is accomplished through a hybrid model, in which stochastic nucleation events are explicitly introduced into the Phase Field model. As a demonstration, this work uses a simple nucleation model to determine local nucleation rates as functions of local supersaturation. These rates are then used to determine the behavior of the nucleation events. This work will limit itself to isothermal processes and will discuss the results in terms of the standard Johnson-Mehl-Avrami-Kolmogorov (JMAK) theory [15–19].

Methods

General reviews of the Phase Field method and its recent applications to solid state transformations are available in the literature [5–8,20–22]. Because of its abilities to treat high volume fractions of ordered phases and coherent strain energy of transformation, this model is ideal for modeling phase transformations in superalloys [23–25]. There have been developments in applying the Phase Field method to incorporate nucleation effects in recrystallization with a constant nucleation rate [26], but to the best of the authors' knowledge, there have been no attempts to adapt the phase field method to processes involving simultaneous precipitation and growth. In this case, it is important to be able to vary the nucleation rate independently, according to the depletion of the matrix, to account for the constantly changing state of supersaturation.

In the usual formulation of the Phase Field model, nucleation is simulated with Langevin noise terms [6]. This provides an elegant treatment of nucleation. However, this becomes computationally expensive, since it requires sampling at a very high frequency in order to observe nucleation events, which are very rare. In the present approach, a nucleation model is maintained as a separate entity from the Phase Field model. The approach is to have two algorithms which alternate, one for nucleation and one for growth and coarsening. The simulation method for nucleation will be discussed in more detail presently; the phase field method will be discussed subsequently.

A. Nucleation

Time and Spacial Scaling. The sample is grided into individual cells, the same cells that are used for the Phase Field method. Nucleation and growth take place by a cyclic process, by which a nucleation phase is followed by a growth phase. During the nucleation phase, nuclei are introduced into individual cells randomly, but with a mean formation rate that matches the desired nucleation rate.

A nucleus forming in an individual cell is modeled as a simple Bernoulli trial. Each cell contains a number of atomic sites, each capable of being a nucleation site. The probability of forming a nucleus at one atomic site in one characteristic nucleation time interval can be calculated by considering the nucleation rate under the classical theory [15,27]:

$$J^* = ZN\beta^* e^{-\Delta G^*/kT} e^{\tau/t} \tag{1}$$

where J^* is the nucleation rate per phase field cell, Z is the non-equilibrium factor due to Zeldovich, N is the number of atoms in each phase field cell, β^* is a frequency factor equal to the reciprocal of the characteristic nucleation time, ΔG^* is the activation energy required to form a stable nucleus, k is Boltzman's constant, T is temperature, τ is the incubation time, and t is the time.

The nucleation rate, on a per atom site basis, is just the quotient J^*/N. This is equal to the instantaneous rate at which nuclei form at atomic sites. If the nucleation rate remains constant over a

$1/\beta^*$ time interval, $J^*/(\beta^* N)$ nuclei will form per atomic site. This process is modeled in this paper with a random number generator that produces a random variable whose value is 1 with probability $p_{1,1}$ and 0 with probability $1 - p_{1,1}$, where $p_{1,1}$ is the probability of forming one nucleus per atomic site in one $1/\beta^*$ time period. Equating the expected value of this random variable with the average number of nuclei formed per site in $1/\beta^*$ time gives:

$$p_{1,1} = \frac{J^*}{\beta^* N}. \tag{2}$$

Since there are, in general, multiple atomic sites within each cell and multiple characteristic nucleation time scales in each Phase Field time step, both time and length dimensions need to be scaled up. For this, it is assumed that nucleation is so infrequent that the event of formation of two nuclei in one cell can be neglected. This is consistent with the usual assumptions made in classical nucleation theory [27]. The further assumption is made that the growth rate of the newly formed nuclei is sufficient that subsequent nucleation of a second precipitate at a later time within a single phase field cell can be neglected.

Making these assumptions, the length scale of $p_{1,1}$ can be increased to give $p_{N,1}$ by calculating the probability that no nuclei form at any of the N sites within the cell in one nucleation time step and then subtracting this from 1. The same reasoning is used to adjust the time scale to that of the Phase Field method by calculating the probability that no nuclei form at *any* of the N sites within the cell for *any* of the M nucleation time steps in one Phase Field time step and subtracting the result from 1. Using these assumptions and the fact that $\beta^* N$ is very large in comparison to J^* gives:

$$p_{N,M} = 1 - e^{-J^* \Delta t_m}. \tag{3}$$

where $\Delta t_m \equiv M/\beta^*$ is just the time allowed for nucleation (Δt_m). Equation (3) is the standard first order decay relationship, which has the reasonable properties that the probability of forming a nucleus becomes zero in the limit as Δt_m does and becomes unity in the limit as Δt_m becomes infinite.

The geometry of the nucleus was chosen to approximate a circle in a discrete lattice. A depletion layer about the nucleus was chosen to be about half as wide as its diameter. The composition was reduced in the depletion layer by exactly the amount required to give the additional solute necessary for the second phase to form in the nucleus. In this way, no solute was introduced into or removed from the system during the nucleation process. This choice of nucleus geometry and composition profile in the depleted zone were made on the basis of simplicity, and produced acceptable answers. Under the more extreme conditions, some numerical problems developed. This is discussed further in the Sample Computations section.

Simple Nucleation Model. A simple model of the nucleation rate as a function of composition was used in order to evaluate the method. Making the following approximations, the nucleation rate was derived: (1) incubation time was neglected throughout, (2) simulations were carried out in 2-D, for which the activation energy for nucleation was $\Delta G^* = \pi\gamma^2/\Delta G_a$, γ is the interfacial energy, and ΔG_a is the free energy change per unit area of the transformation, (3) $\Delta G_a \approx const \times \Delta c$, where Δc is the supersaturation [28]. This gives:

$$J^* = \kappa_1 e \kappa_2 / \Delta c \tag{4}$$

where $\kappa_1 = ZN\beta^*$ and $\kappa_2 = \pi\gamma^2/(const \times kT)$. In the computations, κ_1 and κ_2 were varied in order to study the effect of nucleation rate on the overall transformation kinetics. Equation (4) is a simplifying approximation: more general models can be used, as well as experimental data.

B. Growth and Coarsening

The 2-D Phase Field method was used to model growth and coarsening. The methodology used here was substantially the same as that of Wang and Khachaturyan [23]. This section gives a brief summary of the method used, but the reader interested in greater detail is referred to the original source.

As applied here, the Phase Field method involves integrating two coupled differential equations:

$$\frac{\partial c}{\partial t} = M\nabla^2\left(f_c - \alpha\nabla^2 c + \frac{\delta E_{el}}{\delta_c}\right) + \xi_c \tag{5}$$

$$\frac{\partial \eta}{\partial t} = -L(f_\eta - \beta\nabla^2\eta) + \xi_\eta \tag{6}$$

where, M and L are mobility constants, α and β are gradient energy coefficients that are related to the interfacial energies between the ordered and disordered phases, c and η are the composition and LRO parameter, respectively, f_c and f_η are the derivatives of the local free energy with respect to c and η, respectively, E_{el} is the elastic energy associated with the lattice mismatch between the matrix and precipitate phases, and ξ_c and ξ_η are noise terms representing fluctuations in the alloy c and η, respectively, also known as Langevin noise terms [6]. In this work, ξ_c and ξ_η were set to zero, since the periodic introduction of particles described above accounts for nucleation. Equation (5) is the continuity equation [20] and Equation (6) gives the evolution of the LRO parameter. These were integrated using Euler's method [29].

Following the method outlined in [23], f was expanded in a Landau series about η and c. For the purposes of computations made in this work, E_{el} was set equal to zero. This choice was made in order to compare the simulation results with existing analytical results and does not represent a limitation of the method. In all computations, time has been made dimensionless to give a reduced time by multiplication by $L\Delta f$, where Δf is a characteristic driving force for the transformation [23].

Results and Discussion

Isothermal computations were performed, using the simplified nucleation model described above. Computations were made over a range of nucleation rates, so that they could be compared with JMAK theory [16–19]. All simulations were performed in 2-D, where the Avrami exponents are 1 for site saturation and 2 for constant nucleation [15].

A. Parameters

The gradient coefficients, $\alpha = 0.8$ and $\beta = 0.8$, chosen as representative gradient energy coefficients. The Landau expansion coefficients of the free energy had the following values: $A = 7.5$, $B = 4.0$, $C = 1.0$, $D = 0.5$, $c' = 0.5$, and $c'' = 0.1$, using the notation in [23]. A composition of 0.388, near the middle of the two phase field was used. The equilibrium compositions are 0.1 and 0.926 for disordered and ordered phases, respectively.

B. Computations

Site Saturation Approximation. As a calibration of the method, a sample site saturation computation was made by setting the Langevin noise terms in Equations (5) and (6) large enough to generate approximately 100 nuclei at $t = 5$. The noise terms were then switched off, allowing the microstructure to

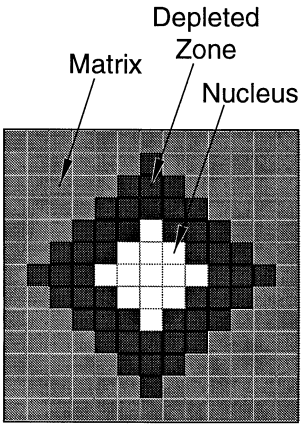

Figure 1. Geometry of nucleus randomly introduced in the microstructure.

evolve with the Phase Field algorithm. Area fractions were determined by segmenting the microstructures about a threshold value of the η for a series of values in order to find a range in which the area fraction was relatively insensitive to the threshold value. Typically, this was approximately half the equilibrium LRO parameter.

An Avrami plot of the *area fraction-time* data was generated by plotting $\ln(\ln\{1/[1 - A_f/A_f^{eq}]\})$ *vs.* $\ln(t)$, where A_f is the area fraction and A_f^{eq} is the area fraction of the product phase at equilibrium. This is shown in Figure 2 and has the expected slope of 1.

Simultaneous Nucleation and Growth. The other extreme was obtained for the present model, by using values of $\kappa_1 = 6.1 \times 10^{-32}$ cell^{-1} and $\kappa_2 = 23.9$, which gave a relatively slow average nucleation rate, where the average nucleation rate is the average of the local rates over all cells. With these values, the average nucleation rate remains within an order of magnitude for a long time and gives an Avrami exponent of 2. Figures 3 (a) and (b) show the Avrami plot and the nucleation rates, respectively, in this case. Figure 4 shows representative microstructures. The average nucleation rate starts at approximately 10^{-6} and slowly drops to approximately 10^{-7} at $t = 100$. This time period in the simulation results in the linear portion of the Avrami curve (Note that $\ln(100) = 4.6$). During this time, the supersaturation is consumed by both nucleation of new particles and by growth of existing ones. For the values chosen for κ_1 and κ_2, J^* is extremely sensitive to small changes in composition, so nucleation is effectively shut down by soft impingement.

The depletion of matrix composition causes the local nucleation rates to decrease, which can be seen by inspection of Equation (4). The rate at which this drop in local nucleation rates occurs is determined by the constant in the exponential, κ_2. Making this constant larger intensifies the effect of solute

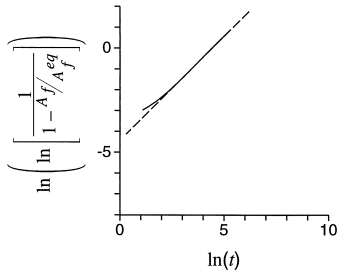

Figure 2. Avrami plot of Phase Field kinetics under site saturation conditions. The dashed line has a slope of unity.

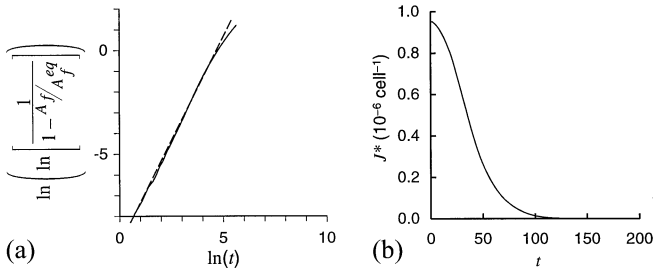

Figure 3. (a) Avrami plot of Phase Field area fraction under slow nucleation conditions. The dashed line has a slope of two. (b) Nucleation rates for the corresponding time.

depletion of the matrix on the local nucleation rates. This causes a steeper decline in average nucleation rate with time, causing the transformation to be closer to site saturation. Making κ_2 smaller makes the local nucleation rates less sensitive to changes in supersaturation, causing the transformation to be closer to the constant average nucleation rate extreme.

The initial values of the local nucleation rates are controlled by the value of κ_1, the pre-exponential factor in Equation (4). Increasing its value causes more nuclei to be formed early on, accelerating the depletion of the matrix of solute. This has the effect of driving the transformation towards the site-saturation extreme, as well. Similarly, decreasing the value of κ_1 causes fewer nuclei to be formed altogether, causing the transformation to be closer to the constant average nucleation rate extreme.

By systematically varying the values of κ_1 and κ_2, it was possible to vary the Avrami exponent from 2 to 1.67, as shown in Figure 5. It was difficult to decrease the Avrami coefficient much beyond 1.67 because of a numerical instability. Essentially, a composition transient develops due to the sharp composition profile for the nuclei. This causes the composition to change enough in the vicinity of the newly formed nucleus to catalyze additional nuclei. A more reasonable composition profile would be diffuse, as predicted by the Cahn-Hilliard theory [30–32]. Work is underway in our group to identify the effects of initial nucleus concentration profile on the transformation kinetics. It is expected that this will solve the instability encountered here.

C. Advantages and Limitations

This model has the advantages of the Phase Field model in that it can account for effects such as large volume fractions, coherent elastic interactions, and ordering in addition to reproducing realistic

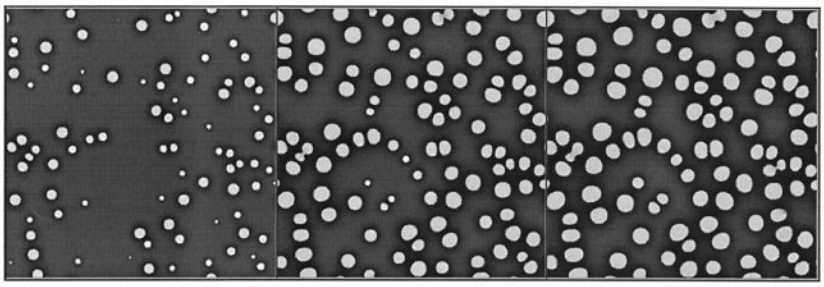

Figure 4. Microstructures formed under slow nucleation conditions. Times in reduced units: (a) 50, (b) 100, and (c) 150.

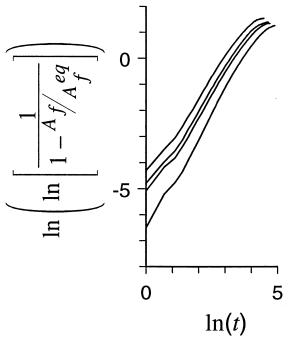

Figure 5. Avrami plots for varying κ_1 and κ_2.

microstructures. Additionally, this work has extended the Phase Field model to transformations involving simultaneous nucleation and growth. However, it is important to remember that there are limitations imposed by the approximations made here. This model only treats homogeneous nucleation and does not account for heterogeneous nucleation. The approximation has been made that two nuclei cannot form adjacent to each other in one nucleation cycle. All computations were made in 2-D, although the algorithm can be extended in a straightforward fashion to 3-D. Finally, all computations have been made under isothermal conditions. This choice was made on the basis of simplicity because the treatment of incubation under non-isothermal conditions remains a difficult problem [33].

Summary

The model presented here explicitly incorporates nucleation events into the Phase Field method, in order to perform simulations of simultaneous nucleation and growth. Since the time scale of forming a nucleus and that of growth differ by orders of magnitude, the conventional Phase Field model is generally used under site saturation conditions or under growth and coarsening conditions alone. This model relaxes this restriction by utilizing a stochastic algorithm, in which nuclei are periodically introduced in the microstructure according to the degree of supersaturation. 2-D simulations of isothermal transformations were made, giving results that were between the extremes of site saturation and constant nucleation predicted by the Johnson-Mehl-Avrami-Kolmogorov (JMAK) theory.

Acknowledgments

The authors would like to express appreciation to Drs. Robert Wheeler and Venkat Seetharaman of UES, Inc., Drs. Lee Semiatin and Dennis Dimiduk of AFRL, and Drs. Dan Backman and Dan Wei of the General Electric Aircraft Engine Group for the helpful discussions regarding the technical aspects of this work. YW and CS would like to express appreciation to NSF for support under contract DMR 9703044. Some of the computations were performed using a grant of HPC time on the SGI Origin 2000 at the US Department of Defense ASC HPC Center at Wright-Patterson AFB.

References

1. J. J. Schirra and S. H. Goetschius, Superalloys 1992, p. 437, TMS, Champion, PA (1992).
2. H. R. Shercliff and M. F. Ashby, Acta Metall. Mater. 38, 1803 (1990).

3. H. R. Shercliff and M. F. Ashby, Acta Metall. Mater. 38, 1789 (1990).
4. H. R. Shercliff and M. F. Ashby, Modelling of the Response of Heat-Treatable Aluminium Alloys to Thermal Processing, Technical Report #PB89–193106/XAB (1989).
5. P. C. Hohenberg and B. I. Halperin, Rev. Mod. Phys. 49, 435 (1977).
6. J. D. Gunton, M. S. Miguel, and P. S. Sahni, in Phase Transitions and Critical Phenomena, ed. C. Domb and J. L. Lebowitz, p. 267, Academic Press, New York (1983).
7. K. Elder, Comput. Phys. 7, 27 (1993).
8. L.-Q. Chen and Y. Wang, JOM. 48, 13 (1996).
9. J. S. Langer and A. J. Schwartz, Phy. Rev. A. 21, 948 (1980).
10. H. Wendt and P. Haasen, Acta Metall. 31, 1649 (1983).
11. R. Kampmann and R. Wagner, in Decomposition of Alloys: the Early Stages, ed. P. Haasen, V. Gerold, R. Wagner, and M. F. Ashby, p. 91, Pergamon Press, New York (1983).
12. R. Wagner and R. Kampmann, in Materials Science and Technology: A Comprehensive Treatment, ed. R. W. Cahn, P. Haasen, and E. J. Kramer, p. 213, VCH, New York (1991).
13. T. P. Gabb, D. G. Backman, D. Y. Wei, D. P. Mourer, D. Furrer, A. Garg, and D. L. Ellis, Superalloys 2000, in press.
14. Y. Wang, H.-Y. Wang, L.-Q. Chen, and A. G. Khachaturyan, J. Am. Ceram. Soc. 78, 657 (1995).
15. J. W. Christian, The Theory of Phase Transformations in Metals and Alloys: Part I, 2nd ed., Pergamon Press, New York (1975).
16. W. A. Johnson and R. F. Mehl, Trans. AIME. 135, 416 (1939).
17. A. E. Kolmogorov, Akad. Nauk. SSR. ISV. Ser. Mat. 1, 355 (1937).
18. M. Avrami, J. Chem. Phys. 7, 103 (1939).
19. M. Avrami, J. Chem. Phys. 8, 212 (1940).
20. Y. Wang, L.-Q. Chen, and A. G. Khachaturyan, in Computer Simulation in Materials Science, ed. H. O. Kirchner, K. P. Kubin, and V. Pontikis, p. 325, Kluwer Academic Publishers (1996).
21. L.-Q. Chen, Scripta Metall. Mater. 22, 115 (1995).
22. V. Tikare, E. A. Holm, D. Fan, and L.-Q. Chen, Acta Mater. 47, 363 (1999).
23. Y. Wang and A. G. Khachaturyan, Scripta Metall. Mater. 31, 1425 (1994).
24. Y. Wang, D. Banerjee, C. C. Su, and A. G. Khachaturyan, Acta Mater. 46, 2983 (1998).
25. D. Y. Li and L.-Q. Chen, Acta Mater. 47, 247 (1999).
26. H.-J. Jou and M. T. Lusk, Phys. Rev. B. 55, 8114 (1997).
27. H. I. Aaronson and J. K. Lee, in Lectures on the Theory of Phase Transformations, ed. H. I. Aaronson, p. 83, TMS, New York (1975).
28. D. A. Porter and K. E. Easterling, Phase Transformations in Metals and Alloys, Van Nostrand Reinhold, New York (1981).
29. W. H. Press, B. P. Flannery, S. A. Teukolsky, and W. T. Vetterling, Numerical Recipes: The Art of Scientific Computing, Cambridge University Press, New York (1986).
30. J. W. Cahn and J. E. Hilliard, J. Chem. Phys. 28, 258 (1958).
31. A. G. Khachaturyan, Theory of Structural Transformations in Solids, Wiley, New York (1983).
32. R. Poduri and L.-Q. Chen, Acta Mater. 45, 245 (1997).
33. Y. T. Zhu, T. C. Lowe, and R. J. Asaro, J. Appl. Phys. 83, 1129 (1997).